Carpathian Journal of Earth and Environmental Sciences, November 2014, Vol. 9, No. 4, p. 61 - 71

THE SOURCE AND EVOLUTION OF METALLOGENIC FLUIDS IN THE DUOBAOSHAN-TONGSHAN PORPHYRY CU (MO) DEPOSIT, HEILONGJIANG, CHINA

Wei HAO[1], Xu JIUHUA[1], Zhang GUORUI[1*], Zeng QINGDONG[2], Liu JIANMING[2], Chu SHAOXIONG[2], & Jiang BAIFANG[3]

*[1]University of Science and Technology Beijing, 30 Xueyuan Road, Haidian District, Beijing 100083 P. R.China; *Corresponding Author: e-mail: ronghaiwei@163.com, Tel. (0086)18701677540*

[2]Institute of Geology and Geophysics Chinese Academy of Sciences, No. 19, Beitucheng Western Road, Chaoyang District, 100029, Beijing, P.R.China

[3]Liaoning Non-ferrous Geological Exploration Institute, No. 7, Beijing Road, Shenhe District, 110013, Shenyang, P. R.China

Abstract: The Duobaoshan-Tongshan porphyry Cu (Mo) deposit, located in the eastern part of the Xingmeng orogenic belt, is the largest porphyry deposit in the Duobaoshan-Aershan Metallogenic belt in central and northern Daxinganling. The ore bodies are mainly hosted inside a granodiorite and at the base of the Duobaoshan Formation. Four ore-forming stages are recognized in the Duobaoshan-Tongshan deposit: (I) Potassic and silicic stage; (II) Silicification-molybdenum mineralizing stage; (III) Phyllic-copper mineralizing stage; and (IV) carbonate-quartz stage. Fluid inclusions of stage (I) are characterized by aqueous, CO_2-H_2O and pure CO_2 fluids, with homogenization temperatures of 245-400◦C, salinities of 6-10 wt%NaCl eqv., and densities of 0.5-0.9 g cm^{-3}. However, those of stage II are dominated by aqueous, CO_2-H_2O, daughter mineral-bearing inclusions, with peak homogenization temperatures of 260-300◦C and salinities of 1.7 - ~39wt%NaCl eqv., and densities of 0.3-1.1g cm^{-3}. Stage III is also characterized by aqueous and CO_2-H_2O inclusions, with peak homogenization temperatures of 200-280◦C, salinities of 0.1-24.8% wt% NaCl eqv., and densities of 0.5-1.0g cm^{-3}. whereas stage IV fluids are aqueous, with homogenization temperatures of 125-170◦C, salinities of 0.5-12.8 wt% NaCl eqv., and densities of 0.8-0.9g cm^{-3}. Respective trapping pressures for stage I, II, and III are 110-160MPa, 58-80MPa, and 8-17MPa, with corresponding formation temperature of 375-650◦C, 310-350◦C, and 210-290◦C. Laster Raman spectroscopic analysis indicates that the main components of the fluid inclusions are H_2O and CO_2. The hydrogen and oxygen isotopic compositions of the fluids responsible for alteration and mineralization are constrained by magmatic fluid and meteoric water, and indicate an evolution process from magmatic hydrothermal fluid to meteoric water-bearing fluid, and indicate the influence of the wall-rocks on the evolution process of the hydrothermal fluids. Microthermometry combined with field observations and fluid inclusion petrography suggest that the Duobaoshan porphyry deposit resulted from magmatic differentiation and the large-scale mixing of distinct fluid types. Moreover, complex structures in the mining area facilitated the transport of the hydrothermal mineralizing fluids and subsequent terminal precipitation. There is a close relationship between copper mineralization and NW-striking foliated shear zones, reflecting the control of later shear belts on the copper mineralization.

Keywords: Duobaoshan-Tongshan, porphyry Cu (Mo) deposit, fluid inclusion, mineralization stage

1. INTRODUCTION

The Duobaoshan-Tongshan porphyry Cu (Mo) deposit, situated in Nengjiang county of the province of Heilongjiang, is the largest porphyry deposit in the Duobaoshan-Aershan Metallogenic belt of Central and northern Daxinganling. Earlier literature on the Duobaoshan deposit has previously described the ore geology, geochemistry, geophysics, geochronology, and metallogeny (Du, 1980; Ma, 1984; Zhao Y.M., et al., 1997; Zhao Y.Y., et al., 1997; Liu et al., 1995; Zhao & Zhang, 1997). Recent publications have

focused on zircon SHRIMP U-Pb ages of the granodiorite in the deposit (Cui et al., 2008), understanding the later reworking of the deposit (Wang et al., 2007), a new understanding of S isotope geochemistry (Feng, 2008), and studies on the original source, signature and enrichment for Cu and Au (Liu et al., 2008). However, studies on the nature of the ore-forming fluid are relatively limited in scope. Li (1979) and Liu et al., (2010) did study fluid inclusions in different quartz veins in the mining area and Wu et al., (2009) conducted a study on fluid inclusions in the Tongshan ore bodies of the Duobaoshan-Tongshan deposit. These studies indicate that mixing and boiling are important mechanisms for Cu-Mo mineralization. However, spatial and temporal links between alteration and mineralization for the different stages of mineralization are absent from these studies. Duobaoshan is an ideal study area for further examination of this problem as its field characteristics, along with ready access to previous documents, have allowed a systematic study of the relationship of spatial distribution and time evolution between hydrothermal alteration and mineralized quartz veins. In this paper, we use new field observations, fluid inclusions data, and stable isotopes (O, H, and S) analysis to refine the roles of the hydrothermal evolution at Duobaoshan, evaluate changes in the hydrothermal fluids and their associated alteration and mineralization as a function of time, establish temperatures and pressures, and indirectly to recognize spatial variations within the deposit, so as to provide new insights to the mineralization.

2. GEOLOGIC SETTING

2.1. Regional geology

The Duobaoshan-Tongshan porphyry Cu (Mo) deposit, in the eastern part of Xing'an-Mongolia orogenic belt, is located between the fold belts of Daxinganling and Jihei (Ge et al., 2007) (Fig. 1). Lithostratigraphic units in the Duobaoshan area are mainly composed of Ordovician, Silurian, Devonian, and Carboniferous lithologies, with lesser amounts of Permian and Jurassic age. The main host to the mineralization, the Ordovician Duobaoshan formation, is composed of intermediate to acid volcanic rocks (Liu et al., 2008; Zhao Y.Y. et al., 1997). Plutonic and volcanic rocks are widespread and mineralization is closely associated with of Hercynian (Du et al., 1988) or early Ordovician age (Cui et al., 2008). NE-striking faults are common in the area and the large-scale, and NW-striking Duobaoshan-Luohe tectonic belt controls the distribution of several deposits, including the Duobaoshan-Tongshan Cu (Mo) deposit.

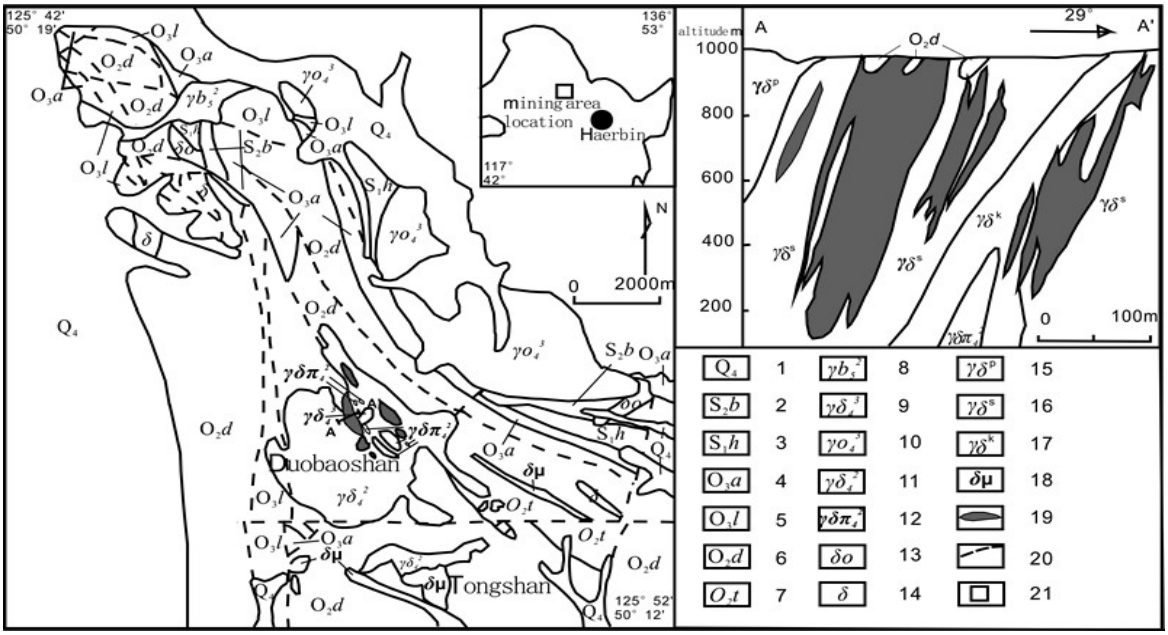

Figure 1. Sketch geological map （left）and a geological profile of Number 3 ore belt (right) of the Duobaoshan-Tongshan porphyry Cu deposit（modified from Du et al., 1988 and Wang et al., 2007）. 1-Quartenary; 2-Middle Silurian Bashilixiaohe Formation; 3- Lower Silurian Huanghuagou Formation; 4-Upper Ordovician Aihui Formation; 5-Upper Ordovician Luohe Formation; 6-Middle Ordovician Duobaoshan Formation; 7-Middle Ordovician Tongshan Formation; 8-Middle Yanshan stage Biotite granite; 9-Late Hercynian oligoclase granite; 10-Late Hercynian Plagiogranite; 11-Middle Hercynian granodiorite; 12-Middle Hercynian granodiorite porphyry; 13-Quartz diorite; 14-Diorite; 15-Propylitic granodiorite; 16-Sericitization granodiorite; 17-Potassium silicification granodiorite; 18-Diorite-porphyrite; 19-Copper ore body; 20-Fault; 21-Location of study area

2.2. Ore Geology

The Duobaoshan-Tongshan porphyry Cu (Mo) deposit was found in 1958 and is currently the third largest copper mine in China. The deposit is a 'super-large' porphyry copper-molybdenum deposit; it is composed of 4 separate ore belts and a total of 215 ore bodies. Mining districts B, C and D 507,840,000 tons of ore and is ranked first in the province for reserves of copper, silver, molybdenum, zeolite, bentonite, marble. The deposit is large, shallow and easy to mine (partly by open-pit mining). Average grades are: 0.47% Cu, 0.016% Mo, 0.144 grams/ton Au, 2.059 grams/ ton Ag. Overall copper content amounts to 2,370,000 tons, of which about 100,000 tons is present as surface/oxidized ore. Other metals include Mo 80,000 tons, Au 73.4 tons and Ag 1046 tons. Primary/hypogene ore accounts for 98% of the deposit whilst the oxidized ore makes up 2%. Potentially harmful elements in the ore include As, F, Pb and Mg.

The Duobaoshan mining district is cut by several groups of faults which appear to control the mineralization, the main ones striking NW-SE and E-W. The former are pre-mineralization and control the most intensive mineralization and alteration zones whilst the E-W-striking faults are general post-mineralization and dissect the ore bodies (Wu et al., 2009; Chen et al., 2009).

The ore bodies are mainly hosted in the sericitization zone with three ore types, including disseminated, disseminated veinlet and veinlet. Ore bodies extend from 0 to 500m away from the porphyry bodies, but the greatest intensity of mineralization occurs in a zone between 50 and 150m from the intrusions. 'Ore' minerals are predominantly comprised of chalcopyrite, pyrite, bornite, and molybdenite, with a zonation from the center to the edge of the ore bodies (bornite to chalcopyrite to pyrite) (Feng, 2008). Gangue minerals mainly consist of quartz, plagioclase, and K-feldspar.

3. ALTERATION AND MINERALIZATION

3.1. Alteration type and zonation

Extensive hydrothermal alteration with evidence of superimposed events are common in many porphyry copper deposits and these features have been recognized at Duobaoshan. The alteration in the central core of the deposit is predominantly pervasive sericitization, from where it grades inwards to a poorly mineralized potassic halo and outwards to a widespread peripheral propylitic alteration with the least amount of mineralization. In addition, a linear phyllic band of alteration, is a later, superimposed alteration type which is related to a NW-striking foliated zone which exhibits the most intense of mineralization.

Petrographic studies of polished and thin sections have complemented the field evidence and resulted in a detailed paragenetic sequence for both silicate and opaque mineral assemblages.

(1) Potash feldspathization (K-feldapr altered to kaolinite) within the porphyry bodies and their intersections with wall rocks, as well as wallrock alteration to the quartz veins (Fig. 2A).

(2) Silicification is widely developed and related to the ore- forming process. Quartz generated by silicification can be subdivided into five types: 1) Quartz accompanied by K-feldspar appears as veins, stockwork-veins and massive, both in metasomatize porphyry and its wall rocks to veins; 2) In epidote-cholrite quartz veins in the propylitic rocks; 3) Quartz veinlets coexisting with molybdenite (Fig. 2B); 4) Grainy quartz superimposed on the phyllic alteration in the foiliated rocks (Fig. 2D) and chalcopyrite-quartz veins (Fig. 2E); 5) Late carbonate-quartz veins (Fig. 2F) .

(3) Sericitization is found in flat, ring – shaped zone between the potassic and propylitic zones (Fig. 3A). Banded phyllic alteration occurs where there is the greatest intensity of foliation (Fig. 3C) and is closely related with chalcopyrite mineralization (Fig. 2E, Fig. 3D).

(4) Propylitization has led to the formation of propylitic andesite and propylitic tuff (Fig. 2B). Proffett (2003) infered that heated meteoric water might be responsible for such propylitization whilst Du et al., (1988) and Lin & Li(1981) have suggested that groundwater heated by intrusion of the porphyry bodies had resulted in the widespread propylitization of wall rocks in the Duobaoshan deposit. It is possible that later volcanism was responsible for development of the epidote-chlorite quartz veins within the andesite and andesitic tuff, but there are epidote-chlorite veins which are cut by veins of chalcopyrite, quartz, calcite and molybdenite (Fig. 2C, F) so it is more likely that these epidote-chlorite quartz veins reflect initial propylitization which occurred prior to porphyry mineralization

(5) Carbonatization occurred after mineralization and led to the development of barren quartz-calcite veins.

3.2. Alteration-mineralization stage

Based on mineral assemblages, crosscuting relationships among distinctive vein types, pervasive alteration patterns and corresponding associated

mineralization, four different stages of hydrothermal alteration-mineralization can be recognized at the Duobaoshan porphyry Cu (Mo) deposit.

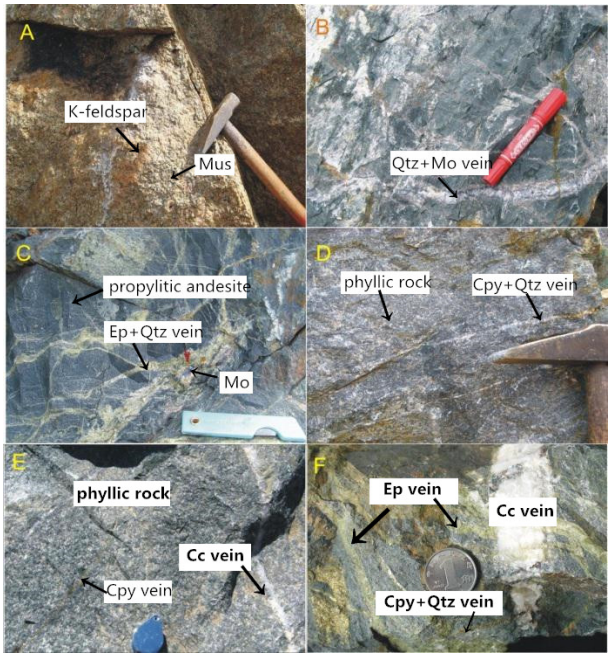

Figure 2. Various veins of different stages in the Duobaoshan-Tongshan Cu (Mo) deposit
A- Epidotization potash feldspathization muscovite granite, DBS011-B 30m, Duobaoshan; B- propylitic andesitic tuff filled by molybdenite-quartz vein; C- propylitic andesite and molybdenite vein filling in Epidote-quartz vein; D-Chalcopyrite veinlets and disseminated copper mineralization in Phyllic rock; E-Chalcopyrite veinlets in Phyllic rock; F- Calcite-quartz vein crosscutting the epidote veins and chalcopyrite quartz vein. Mus-muscovite; Qtz-quartz; Mo-molybdenite; Ep-epidote; Cpy-chalcopyrite; Cc-calcite.

The potassic and silicic stage (I) is characterized by an assemblage of K-feldspar and quartz and corresponds to the earliest stage of alteration. It occurs mainly within the porphyry bodies and their contacts with wall rocks as well at the margins of quartz veins (Fig. 2A); it also appears in the muscovite granite pluton and andesite. Potassic alteration occurs as a replacement of both plagioclase phenocrysts and groundmass by K-feldspar and occurs as vein-shaped, stockwork-shaped and massive features replacing the host rock. In general, copper mineralization is weak in this stage, but does occur within quartz veins as fine-grained aggregates and disseminated crystals. Propylitic alteration seems to occur in association with all the mineralizing stages. It is observed mainly as selective alteration of mafic minerals and forms chlorite-epidote-calcite filledfractures in the andesite. In the pit area, it is pooly developed, but appears to be contemporaneous with potassic alteration. In addition, more pervasive propylitic alteration within the andesite and andesitic tuff is recognized to be a result of later volcanism and many epidote-chlorite veins are cut through by veins of chalcopyrite-quartz, molybdenite-quartz and calcite (Fig. 2C, F); it is therefore inferred that these epidote-chlorite quartz veins probably reflect initial propylitization prior to porphyry mineralization.

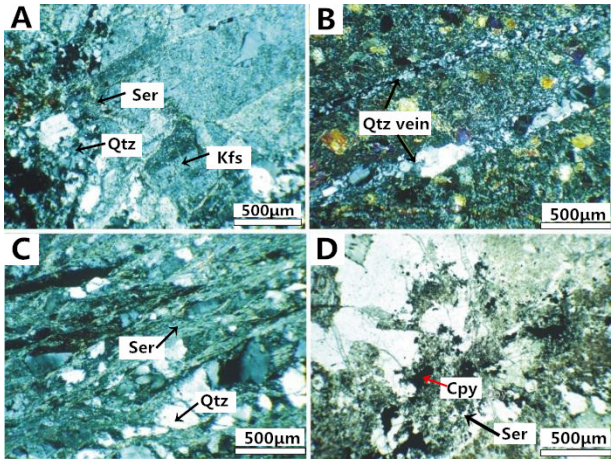

Figure 3. Characteristics of mineralization and alteration in Duobaoshan-Tongshan Cu (Mo) deposit
A- K-feldspar altered granodiorite porphyry superimposed by phyllic alteration, DBS044, (+); B- Stockwork silicification of propylitic andesite, DBS049, (+); C-Phyllic granitic mylonite, (+); D- Cataclastic granodiorite porphyry superimposed by phyllic alteration, Chalcopyrite, DBS053, (-).Ser-sericite; Qtz-quartz; Kfs-K feldspar; Cpy-chalcopyrite.

Silicification-molybdenum mineralizing stage (II) is characterized by an assemblage of molybdenite and quartz. Most of the Mo is deposited after stage I, along with lesser chalcopyrite. This stage often infills veins of K-feldspar-quartz or epidote-quartz as a scaly aggregate (Fig. 2B, C). Molybdenite veins are often cut by later veins of chalcopyrite, carbonate, sericite and quartz in the foliated rocks. Lesser molybdenite is distributed as disseminations along joints within the foliated zones, and has often suffered deformation.

The phyllic-copper mineralizing stage (III) is characterized by an assemblage of chalcopyrite-pyrite-bornite-quartz, and occurs in veinlets that commonly cut the former two stages. Sericitic alteration is generally superimposed on the potassic and propylitic alteration as a pervasive replacement of mainly plagioclase phenocrysts and groundmass, and is closely related with chalcopyrite mineralization (Fig. 2E, Fig. 3D). The linear phyllic band, a later alteration corresponding to a NW-striking foliated zone, is superimposed on the sericitic alteration and exhibits the largest intensity of mineralization, which then gradually decreases in

intensity outwards. Chalcopyrite - (pyrite) - quartz veins can be observed mostly in the fractures of the phyllic and propylitic altered rocks. Two Cu mineralizing events have been recognised: chalcopyrite mineralization occurring before the foliation stage is mostly restricted to around porphyry pluton, while the later copper mineralization which was emplaced after the foliation stage occurs along foliated joints as fine grains or veinlets coexisting with phyllic and sericite alteration (Fig. 2D).

The carbonate - quartz stage (IV) is characterized as a post-mineralization assemblage of quartz and calcite veins containing no ore mineralization.

4. FLUID INCLUSIONS

Representative samples of quartz veins from various stages selected from the open-pit of Duobaoshan-Tongshan mines were selcted for fluid inclusion study. Thermometric data exhibited in Table 2 were gathered from approximately 555 fluid inclusions host in quartz. Microthermometry was performed at the Fluid Inclusion Laboratory of Resource Engineering Department, University of Science & Technology Beijing, using a LinKman THMS-600 heating-freezing stage, with a temperature range of -196°C - +600°C. Salinities for L-V type inclusions were calculated using the formula of Hall (1988) and the salinity-ice relationship of Bodnar (1993). Densities are estimated using the formula from Bodnar (1983). Salinities for CO_2-H_2O type inclusions were calculated from the formula from Roedder (1984) and densities using the formula from Liu & Shen (1999) as well as Shepherd et al's (1985) diagram of relationships between CO_2 homogenization and CO_2 density.

4.1. Fluid inclusion petrography

Fluid inclusions can be classified into several general types based on their phase composition at room temperature.

Type L-V (liquid-rich) fluid inclusions are the most common and consist of two phases at room temperature: liquid and a vapor bubble (Fig. 4A), the liquid amounting to >50 percent of cavity volume. They occur as groups or in isolation as ellipse-shaped, irregular forms and negative crystals in all the stages, and have sizes in the range 3-15 μm, sometimes up to 20 μm. Some of them are arranged in trails in healed microfractures or along former and present quartz grain boundaries, whilst others with a linear configuration crosscut grain boundaries. The occurrence of inclusions along growth zones of quartz crystals suggests a primary origin, while the crosscutting relationships reflect overprinting of a secondary fluid. On heating, these homogenize into the liquid phase.

Type V-L (vapor-rich) inclusions also consist of liquid and vapor but contain more than 50 percent of vapor by volume; they mostly homogenize into the vapor phase. They are mostly present as primary inclusions in stage III mineralization.

Type CO_2-H_2O (CO_2-rich) inclusions consist mostly of liquid CO_2 and liquid water at room temperature, occasionally plus vapor CO_2 (Fig. 4D,F). Sizes range from 2-20 μm and CO_2/H_2O ratios are variable (0.1 to 0.9). These inclusions occur as isolated ellipses or irregular clusters, with no planar orientation, in stages I, II, III, and appear to have a primary origin.

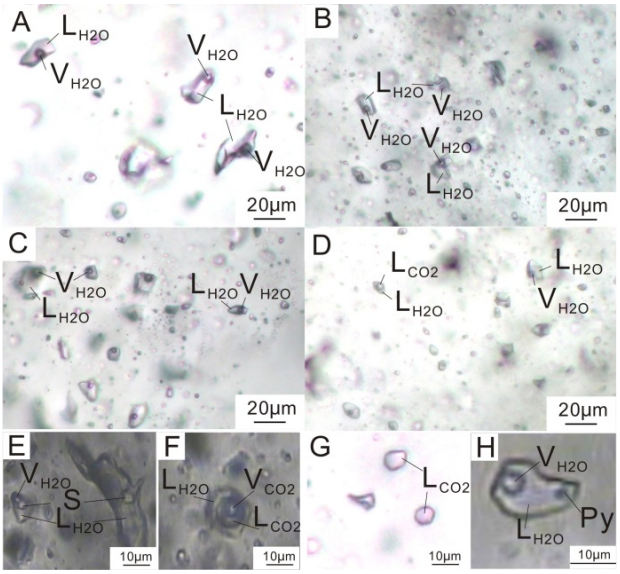

Figure 4. Micrographs of fluid inclusions in the Duobaoshan-Tongshan porphyry Cu (Mo) deposit
A-Chalcopyrite-quartz vein, primary inclusions, DBS002; B-L-V inclusions in quartz vein at side of azurite-chalcopyrite quartz vein, DBS003; C-Chalcopyrite-quartz vein, L-V inclusions with different vapor-liquid ratios in quartz at side of chalcopyrite, DBS023A; D-The coexistence of L-V and L_{CO2}-L_{H2O} inclusions in chalcopyrite -quartz vein, DBS025; E-Isolated L-V-S type inclusions in molybdenite-quartz vein, D101; F- CO_2-H_2O type (V_{CO2}+ L_{CO2}+L_{H2O}) inclusions in molybdenite-quartz vein, D101; G-L_{CO2} type inclusions in early quartz veins of sericitolite, DBS017A; H- sulfide-bearing inclusions in quartz vein of granodiorite porphyry , DBS065; L_{CO2} -Liquid phase CO_2; V_{CO2}- Vapor CO_2; S-Halite; L_{H2O}-Liquid phase water; V_{H2O}-Vapor phase water; Py-Pyrite.

Type CO_2 (pure CO_2) inclusions contain only

liquid CO_2 or vapor CO_2 at room temperature(Fig. 4G). They are relatively scarce and occur as primary inclusion in stages I and III, sometimes closely intergrown with CO_2-H_2O inclusions.

Type L-V-S inclusions (multiphase) contain liquid, vapor and crystalline phases. The most common solid phase cubic halite (NaCl) (Fig. 4E). A few inclusions contain an opaque phases whose X-ray energy spectrum analysis reveal the presence of Fe and S (Fig. 4H). Type L-V-S inclusions are rare but occur as isolated ellipses in stage II mineralization.

4.2. Microthermometric measurements

Most of the microthermometric measurements were conducted on primary inclusions, characterized by their presence in crystal growth zones or by their occurrence as isolated inclusions with no visible relationship to other nearby inclusions. A small number of secondary inclusions that delineate healed fractures within the quartz crystals were also studied.

Fluid inclusions in stage I are characterized by aqueous water, CO_2-rich and (lesser amounts of) pure CO_2 inclusions, with a higher homogenization temperature range of 245-400°C, salinities of 1.7-11.7wt%NaCl eqv., and densities of 0.5-0.9g·cm^{-3}. Fluid inclusions with different vapour-liquid ratios generally homogenize to liquid at widely variable temperatures, pointing to a continuous variation in compositions or densities of the fluids during the mineraliztion process. For example, fluid inclusions with different CO_2/H_2O ratios will have different proportions of vapor and different homogenization temperatures even though they were trapped at identical temperature and pressure. In this situation, the higher homogenization temperatures are closer to the trapping temperature (Shepherd et al., 1985). Total homogenization temperatures of CO_2-H_2O type fluid inclusions are concentrated in the range 360-380°C, and partial homogenization temperatures, salinities and densities are -7.5 - +30°C, 6%-10% and 0.6-0.9 g·cm^{-3} respectively.

L-V type, CO_2-H_2O type and L-V-S type inclusions occur in stage II. Some of the CO_2-H_2O types homogenizing to liquid CO_2 coexist with aqueous inclusions which homogenize to liquid water. In addition, some inclusions are characterized by the coexistence bewteen daughter mineral-bearing inclusions and L-V type inclusions which homogenize to vapour or liquid, providing evidence for localized CO_2-H_2O immiscibility. On heating, daughter minerals disappear both earlier and later than liquid-vapour homogenization. Peak homogenization temperatures of L-V type inclusions are concentrated over two intervals: 135-175°C and 260-300°C, the former interval being related to later hydrothermal activity, while the latter corresponds to the main alteration-mineralization fluid. Salinities of L-V type inclusions concentrate in the ranges 1-6% and 12-23%, and densities are 0.7-1.1 g·cm^{-3}. CO_2-H_2O type inclusions are characterized by total homogenization temperatures around 280-300°C, CO_2 partial homogenization temperatures of 28.2 - 32.4°C, salinities of 2%-6% and densities of 0.3-0.7g·cm^{-3}. The rarer L-V-S type inclusions have a homogenization temperature range from 265 to 310°C and salinities from 35%-39%.

Inclusions in stage III are characterized by L-V type, CO_2-H_2O type, and a few of L_{CO2} type, and exhibit CO_2-H_2O immiscibility as well as characteristics indicative of boiling (L-V inclusions which homogenize to liquid and vapour over a similar homogenization temperature range within the same field of view). Homogenization temperatures of L-V type inclusions also show two intervals (130-165°C, 200-280°C); the low temperature interval of 130-165°C largely relates to secondary, later hydrothermal fluid activity to some extent, while the temperature interval from 200 to 280°C is most likely the minimum ore forming temperature range for this stage of alteration-mineralization. Salinities and densities range from 0.1 to 24.8% and 0.5-1.0g·cm^{-3} respectively. Inclusions of CO_2-H_2O type display a homogenization temperature range of 260-280°C, CO_2 partial temperatures between 26.4-29.6°C, salinities from 6-10% and densities in the range 0.6-0.7 g·cm^{-3}.

Inclusions in stage Ⅳare withal of L-V type. Homogenization temperatures are between 125-170°C, salinities are 0.5%-12.8% (mostly 4-10%) and densities are 0.8-0.9g·cm^{-3}.

Notwithstanding the influences from secondary fluids, it is clear that both the molybdenum mineralization stage and the copper mineralization stage are characterized by relatively high homogenization temperatures although progressively changing compositions and densities for the ore-forming fluids are also noted.

4.3. Laster Raman spectroscopic analysis

Laster Raman spectroscopic analysis was carried out in the Geological Education Center of the Earth and Spatial Science Institute, Peking University. Equipment used was a Renishaw RM-1000, using 514nm radiation emitted from an Ar+ laser, spectrum, a count of 10 second, a resolution of 1-2cm^{-1}, and laser spot of 1-2μm. The

results of the analyses indicate the presence of large numbers of H_2O-bearing and CO_2-bearing inclusions, as well as some pure CO_2 inclusions (Fig. 5). Type L-V inclusions are characterized by vapor H_2O, liquid H_2O and CO_3^{2-}, with peaks at 3390~3500cm^{-1}and 1065 cm^{-1}. Pure CO_2 inclusions, mainly contain vapour CO_2 or minor amounts of liquid CO_2 with Raman peaks at 1386 and 1282cm^{-1}. Type CO_2-H_2O inclusions are mostly recognized as an assemblage of liquid CO_2, vapour CO_2, and liquid H_2O, with respective Raman peaks at 1386, 1282 and 3400cm^{-1}. In summary, the ore-forming fluid in the Duobaoshan-Tongshan deposit, is composed of CO_2-NaCl-H_2O for the early stage and NaCl-H_2O for the late stage, and is thus similar to fluids from other such porphyry copper deposits (Li N, et al., 2007; Li G.M., et al., 2007).

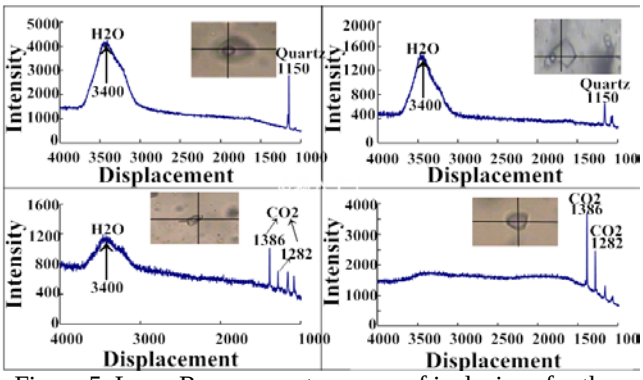

Figure 5. Laser Raman spectorgrams of inclusions for the Duobaoshan-Tongshan porphyry Cu (Mo) deposit
A-Vapor phase compositions of L-V type inclusion, DBS039; B-Liquid phase compositions of L-V type inclusion, DBS033; C-CO_2 phase of CO_2-H_2O type inclusion, DBS066; D-compositions of LCO_2 type inclusion, DBS039

4.4 Isotope analysis

10 samples of quartz which was used for inclusion study, were also analysed for their isotopic compositions of both O for quartz and D for fluid inclusions (Table 1).

The calculated δD range of extracted fluid is from -101.5 to -82.2 per mil. The $\delta^{18}O$ composition of water coexisting with quartz at the derived trapping temperatures indicated by fluid inclusions was calculated from the equation $1000\ln\alpha\ (Q\text{-}H_2O) = 3.306\times10^6T^{-2} - 2.71$ (Zhang, 1989), and results fall in the range -3.02 to 8.35 per mil. δD and $\delta^{18}O$ ranges of water in equilibrium with stage I quartz are -94.4 to -95.5 and 7.6 to 8.1 per mil, respectively, water in equilibrium with stage III quartz has δD values of -82.2 to -101.5 and $\delta^{18}O$ values of 2.0 to 3.4 per mil.

5. DISCUSSION

5.1. Trapping temperatures and pressures

The pressures of the fluid inclusions at homogenization represent minimum trapping pressures and are only equal to the trapping pressures under conditions of boiling (Roedder & Bodnar 1980). The trapping pressure of the CO_2 type inclusions and coexisting aqueous inclusions with low salinities in stage I can however be more precisely calculated to be 110-160 MPa, according to the H_2O - CO_2 P-T diagram provided by Roedder & Bodnar (1980). Applying the method of CO_2 concentration (He, 1982) in conjunction with a CO_2-H_2O diagram suggests a trapping pressure of approximately 58-80 MPa for 3-phase CO_2-H_2O type inclusions in stage II; homogenization pressures of local L-V-S type inclusions in this stage range from 20 to 70 MPa. The abundant boiling inclusions in stage III can be constrained from the diagrams of Bodnar & Vityk(1994), Diamond (2001), and Roedder & Bodnar (1980); these boiling inclusions have a trapping pressure range of 8-17MPa.

Table 1. Isotopic compositions of hydrogen and oxygen for the ore forming fluids of the Duobaoshan-Tongshan deposit

Alteration-mineralization stage	Sample number	calibrated temperature (°C)	δO_{quartz} (‰, VSMOW)	δD_{H2O} (‰, VSMOW)	Calculated $\delta^{18}O_{H2O}$ (‰, VSMOW)
Stage Ⅲ	DBS002	250	11.8	-85.9	2.4
Stage Ⅲ	DBS004	250	12.0	-101.5	2.6
Stage Ⅲ	DBS17b	250	11.9	-94.0	2.5
Stage Ⅲ	DBS023	250	11.4	-82.2	2.0
Stage Ⅲ	DBS025	250	12.2	-87.1	2.8
Stage Ⅲ	DBS027	250	11.9	-93.1	2.5
Stage Ⅲ	DBS030	250	12.8	-99.5	3.4
Stage Ⅲ	DBS039	250	12.1	-86.2	2.7
Stage Ⅰ	DBS019	500	10.4	-95.5	7.6
Stage Ⅰ	DBS043	500	10.9	-94.4	8.1

Analysed at the Nuclear Industry Geological Research Institute, Beijing. Data values are based on the international standard V-SMOW, type of mass spectra: MAT-253.

There are large numbers of L-V type inclusions in all of the stages; on the basis of both NaCl-H_2O characteristics (Zhang & Frantz, 1987) and the NaCl-H_2O P-T diagram for different salinities (Bodnar & Vityk, 1994) their maximum homogenization pressures show a gradual decrease from 100 MPa in the early stages to 5 MPa in the later stages .

According to these calculated pressures and a suggested rock density of 2.72g cm^{-3} (Ji et al., 1989), it is likely that depths of mineralization were around 4.0-5.8 km (for lithostatic pressure) in stage II and 0.84-1.68km (for hydrostatic pressure, because of boiling) in stage III. After applying corrections for pressure and salinity it can be concluded that the formation temperatures for the main alteration-mineralization stages are as follows: 375-650°C (coinciding with 509°C calculated by isotope geothermometry; Du Qi, 1988) for stage I, 310-350°C for stage II, 210-290°C for stage III (220-340°C obtained by isotope geothermometry; Ma Deyou, 1984). Furthermore, the P-T diagram for boiling (Hass, 1976) a depth for mineralization for stage III of 0.6-1.4 km.

5.2 The source of metallogenic fluid

Ore-bearing fluids may derive from hot brine, connate, meteoric water, metamorphic water and magmatic water etc, while, the isotopic composition of hydrogen and oxygen in these waters are recognized as one certain tracer for different hydrothermal fluids.

According to hydrogen and oxygen isotopic compositions for different stages, $\delta\ ^{18}O$- δ D isotopic projection diagram are obtained (Fig. 6), which describes that hydrogen and oxygen isotopic compositions for different metallogenic fluids are located between magmatic water and meteoric water, With hydrogen and oxygen projection points showing below the magmatic water, hydrothermal fluids in the potassium silicification stage (stage I), mainly magmatic water, reflect an influence on hydrothermal fluids made by process of water-rock interaction at high temperature; for phyllic-copper mineralizing stage(stage III), hydrogen and oxygen isotope projection points shift evidently toward meteoric water, which indicate amounts of meteoric water joining into the alterated hydrothermal fluids. Therefore, above mentioned features generally show an evolution process from magmatic hydrothermal fluid to a mixing magmatic and meteoric fluid, meanwhile, imply wall-rock's influences on the evolution process of hydrothermal fluids.

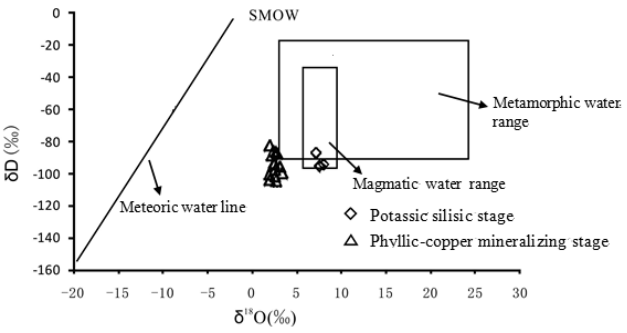

Figure 6. Isotopic projection diagram bewteen hydrogen and oxygen for Duobaoshan-Tongshan deposit

5.3 Fluid evolution in stage I and stage II

Nash (1976) held that there were two kinds of inclusions showing respectively high (salinity>30%, temperature>400°C) and moderate (salinity: 10%-25%, temperature: 200-400°C) S-T condition in the porphyry deposit. Also, Misra (2005) summarized world-famous porphyry deposits and concluded that homogenization temperatures of fluid inclusions were generally 200-600°C in the porphyry deposit, and salinities of <5% to >60%. Moreover, from Rui et al., perspective(2003), 100-980°C and 2-64% for those of porphyry deposit respectively. Compared to above listed data, the ore-forming temperatures of Duobaoshan-Tongshan deposit are approximately identical but a relatively low range for salinities. Likewise, it can be illustrated by figure 7 that shows a gradually decreasing trend in homogenization temperature from early stage to late stage. It will be more obvious for the decreasing trend to use revised forming temperatures.

Lowenstern (2001) and Halter & Webster (2004) suggested that CO_2-bearing fluid with high temperature and intermediate-low salinity can be yield directly by differentiation of Intermediate-acid magma. Fluids in stages I are characterized by CO_2-bearing, relatively high temperatures and intermediate-low salinity of 6-10%, therefore, fluids in this stage may be regarded as a result of late differentiation of magma. As described in the figure 7, the majority of inclusions in stages I are close to supercritical range. If homogenization temperatures were replaced by formation temperatures, more inclusions would enter into the supercritical range. In view of the above points, fluids in this stage may represent supercritical fluids originated from magma. However, pressures in this stage are so large (110MPa-160MPa) that it is hardly feasible to make supercritical fluids immiscible during the process of ascending. Therefore, the features of immiscible fluid inclusions are not observed.

CO_2-rich inclusions are obviously increasing in stage II, both their formation temperatures (310-350°C) and pressures (58-80MPa) fall to immiscible range between CO_2 and H_2O. A great deal of inclusions homogenizing to liquid-phase CO_2 or vapour-phase CO_2 in this stage are observered and coexist with inclusions homogenizing to liquid-phase H_2O, which indicates a immiscibility between CO_2 and H_2O before they are trapped (Roedder, 1984), and plenty of CO_2 break away from brine, that is, some inclusions, as immiscible phases, are heterogeneously trapped in this stage (Lu et al., 2004). Due to the immiscibility of fluid (Lowenstern, 2000), there are two completely distinct salinity ranges for CO_2-H_2O type inclusions and L-V type inclusions. While, the immiscibility do not lead in a sharp decline, even supersaturation virtually in the salinity, instead, result in extremely small quantities of halite crystal-bearing inclusions in certain location.

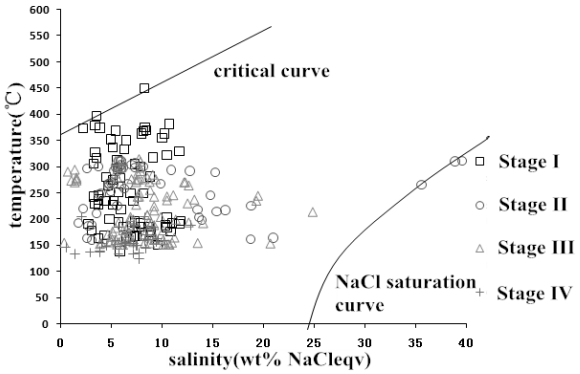

Figure 7. Temperature- salinity diagram of inclusions for Duobaoshan-Tongshan porphyry Cu (Mo) deposit.

5.4 Fluids evolution in stage III

Ore-forming temperatures, pressures (8-17MPa) and the number of CO_2-rich inclusions become smaller gradually in stage III, which are probably attributed to the large number of CO_2 escaping from brine at the same time, CO_2 and other acid volatile components escaping from brine can also result in growth of pH. Inclusions in this stage are evidently characterized by increasing vapour-rich inclusions generally homogenizing into vapour phase, which are distinguished from those in stage II. In addition, L-V type inclusions show intense boiling feature: homogenizing into vapour and liquid phase respectively in one field of view within similar homogenization temperature range. However, relatively low salinities (focusing on 6%-12%) are different from intense boiling feature, the reason for which may be that temperature and pressure can change rapidly when fluids at high temperature encounter groundwater or rainwater at lower temperature, as a result, fluids begin to boil, but, trapped inclusions in this case are only characterized by vapour-bearing or liquid-beraing L-V type inclusions rather than L-V-S type inclusions with high salinities (Liu & Shen, 1999; Qiu et al., 2001). Consequently, besides sharp decline in pressure, different mixing fluids are responsible for intense boiling with a relativey low salinity. This point can also be illustrated by hydrogen and oxygen isotope of quartz vein in the stage III.

As studied on the inclusions in mineralizing stages, it's suggested that besides magmatic differentiation, large scale of distinct mixing fluid should also play a significent role in the mineralizing process of hydrothermal fluids. Moreover, complex structure fractures in the mining area bring great conveniences for mineral-bearing hydrothermal fluids to transfer as well as store minerals, with the gradually transformation of temperature, sharp decline in the pressure, alteration of composition, and other changes in the physical and chemical conditions, mineral-bearing hydrothermal fluids produce relatively intense immiscibility and boiling during the process of runing through structure fractures, so as to arouse precipitation of minerals, in the end, establish a superlarge porphyry Cu (Mo) deposit.

6. CONCLUSIONS

(1) Alteration and mineralization process of the Duobaoshan-Tongshan porphyry Cu (Mo) deposit can be divided into four stages from early to late stage: Potassium silicification stage (I); silicification-molybdenum mineralizing stage (II); phyllic-copper mineralizing stage (III); and carbonate-quartz stage (IV), of which, stage II, III are main metallogenic stages for Mo, Cu, there are lesser amounts of mineralization in the stage I, and almost no mineralization in the stage IV.

(2) Fluid inclusions of stage (I) are characterized by aqueous, CO_2-H_2O and pure CO_2, with homogenization temperatures of 245-400°C, salinities of 6-10 wt% NaCl eqv., and those of stage II is dominated by aqueous, CO_2-H_2O, daughter mineral-bearing inclusions, with peak homogenization temperatures of 260-300°C and salinities of 1.7~39wt%NaCl eqv. Stage III is also characterized by aqueous and CO_2-H_2O inclusions, with peak homogenization temperatures of 200-280°C, salinities of 0.1-24.8% wt%NaCl eqv., whereas stage IV is simply aqueous, with homogenization temperatures of 125-170°C, salinities of 0.5-12.8 wt%NaCl eqv..

(3) Hydrogen and oxygen isotope of the fluids for stage I and III are constrained by magmatic water and meteoric water, which indicate an evolution process from magmatic hydrothermal fluid to a mixing magmatic and meteoric fluids.

(4) Respective trapping pressure for stage I, II, III are 110-160MPa, 58-80MPa, 8-17MPa, corresponding formation temperature are 375-650°C, 310-350°C, 210-290°C. Homogenization temperatures and homogenization pressures exhibite a gradually decrease toward the late stage.

(5) Duobaoshan porphyry deposit is a complex structure-magma ore forming system: mineral-bearing hydrothermal fluids are not only derived from magmatic differentiation; large scale of distinct mixing fluids should also play a significant role; complex structure fractures in the mining area bring great conveniences for mineral-bearing hydrothermal fluids to transfer as well as store minerals.

ACKNOWLEDGEMENTS

Fieldwork for this study was aided and supported by the Duobaoshan mining company. The authors are very grateful to Wang Yongbin from the Institute of Geology and Geophysics, Chinese Academy of Sciences, and Chai Hui from the China University of Geosciences (Beijing) for their continuous help during the fieldwork.

REFERENCES

Bodnar, R.J. 1983. *A method of calculating fluid inclusion volumes based on vapor bubble diameters and PVTX properties of inclusion fluids*. Econ Geol, 78: 535-542.

Bodnar, R.J. & Vityk, M.O. 1994. *Interpretation of microthermometic data for H_2O-NaCl fluid inclusions*. In：de Vivo B, Frezzotti M L. Fluid Inclusions in Minerals: Methods and Applications. Blackberg: Verginia Tech. 117-130.

Bodnar, R.J. 1993. *Received equation and table for determining the freezing point depression of H_2O-NaCl solution*. Geochim Cosmochim Acta, 57: 683-684.

Chen, Y.J., Zhai, M.G. & Jiang, S.Y. 2009. *Significant achievements and open issues in study of orogenesis and metallogenesis surrounding the North China contient*. Acta Petrologica Sinica, 25(11): 2695-2726 (in Chinese with English abstract).

Cui, G., Wang J.Y.，Zhang, J.X. & Cui, G. 2008. *U-Pb SHRIMP dating of zircons from Duobaoshan granodiorite in Heilongjiang and its geological significance*. Global Geology, 127(14): 387-394 (in Chinese with English abstract).

Diamond, L.W. 2001. *Review of the systematic of CO_2-H_2O fluid inclusions*. Lithos, 55: 69-99.

Du, Q.，Zhao, Y.M.，Lu, BG，Ma, D.Y.，Li, P.L.，Lv, J.K.，Li, W.S.，Ao, Z.L. & Cui, G. 1988. *Porphyry Cu deposit Duobaoshan*. Beijing: Geology Publishing House, 1-334 (in Chinese).

Du, Q. 1980. *The alteration and mineralization features of the Duobaoshan porphyry copper deposit*. Acta Geologica Sinica, 4: 310-323 (in Chinese with English abstract).

Feng, J.H. 2008. *Distribution character of sulfur isotope in the Duobaoshan deposit*. Geology and Prospecting, 44(1): 46-49 (in Chinese with English abstract).

Ge, W.C.，Wu, F.Y.，Zhou, C.Y. & Zhang, J.H. 2007. *Porphyry Cu-Mo deposits in the eastern Xing 'an-Mongolian Orogenic Belt*: Mineralization ages and their geodynamic implications. Chinese Science Bulletin, 52(18): 2097-2105 (in Chinese with English abstract).

Hall, D.L.，Sterner, S.M. & Bodnar, R.J. 1988. *Freezing point depression of NaCl-KCl-H_2O solutions*. Econ Geol, 83: 197-202.

Halter, E.W. & Webster, D.J. 2004. *The magmatic to hydrothermal transition and its bearing on ore forming systems*. Chemical Geology, 210: 126.

Hass, J.L. 1976. *Physical properties of the coexisting phases and thermochemical properties of the H_2O component in boiling NaCl solutions*. U S Geol Surv Bull, 1421A: 1-73.

He, Z.L. 1982. *Inclusion mineralogy*. Beijing: Geology Publishing House, 86-92 (in Chinese).

Ji, K.J.，Wu, X.H. & Zhang, G.B. 1989. *ore deposits Source，water source and heat source of hydrothermal deposit and its distribution feaure*. Beijing: Science and Technology Publishing House, 3-22 (in Chinese).

Misra, K.C. 2005. *Understanding mineral deposit*. Dordrecht: Kluwer Academic Publishers, 397-418.

Li, G.M., Li, J.X., Qin, K.Z., Zhang, T.P. & Xiao, B. 2007. *High temperature，salinity and strong oxidation ore-forming fluid at Duobuza gold-rich porphyry copper deposit in the Bangonghu tectonic belt，Tibet: Evidence from fluid inclusion*. Acta Petrologica Sinica, 23(5): 935-952.

Li, K.S. 1979. *Research on gas-liquid inclusions of Duobaoshan Porphyry Cu-Mo deposit.* Geology and Prospecting, (3): 22-23 (in Chinese with English abstract).

Li, N., Chen, Y.J.，Lai, Y. & Li, W.B. 2007. *Fluid inclusion study of the Wunugetushan porphyry Cu-Mo deposite, Inner Mongolia*. Acta Petrologica Sinica, 23(9): 2177-2188 (in Chinese with English abstract).

Lin, J.Q. & Li, G.L. 1981. *Rock alteration mechanism of Duobaoshan porphyry copper deposit*. Journal of Jilin Unviersity: (Earth Science), (2): 35-41 (in Chinese).

Liu, B. & Shen, K. 1999. *Fluid Inclusion*

Thermodynamics. Beijing: Geologyical Publishing House, 70-118 (in Chinese).

Liu, C., Mu, Z.G., Liu, R.X. & Huang, Y.L. 1995. *$^{40}Ar/^{39}Ar$ laster microprobe dating on hydrothermal minerals from Duobaoshan porphyry copper mining district, Heilongjiang province, China*. Geological Sciences, 30(4):330-337 (in Chinese with English abstract).

Liu, J., Wu, G., Zhong, W. & Zhu, M.T. 2010. *Fluid inclusion study of the Duobaoshan porphyry Cu(Mo) deposit, Heilongjiang Province, China.* Acta Petrologica Sinica, 26(5): 1450-1464 (in Chinese with English abstract).

Liu, Y., Cheng, X.Z., Wang, X.C., Liu, J.Y., Wang, L. & Wang, X.L. 2008. *Cu source and enrichment laws of the Duobaoshan porphyry copper deposit in Heilongjiang province.* Chinese Journal of Geology, 43(4): 671-684 (in Chinese with English abstract).

Lowenstern, B.J. 2000. *A review of the contrasting behavior of two magmatic volatiles, chlorine and carbon dioxide.* Journal of Geochemical Exploration, 69-70: 287-290.

Lowenstern, B.J. 2001. *Carbon dioxide in magmas and implications for hydrothermal systems.* Mineralium Deposita, 36: 490-502.

Lu, H.Z., Fan, H.R., Ni, P., Ou, G.X., Shen, K. & Zhang, W.H. 2004. *Fluid Inclusion*, Beijing: Science Press, 168-169 (in Chinese).

Ma, D.Y. 1984. *Isotope geology of the Duonaoshan copper ore field.* Mineral Deposits, 3(1): 47-57(in Chinese with English abstract).

Nash, J.T. 1976. *Fluid inclusion petrology data from porphyry copper deposits andapplication to exploration*. US Geol Survey Prof Paper 907-D, 1-16.

Proffett, J.M. 2003. *Geology of the Bajo de la Alumbrera porphyry copper-gold deposit, Argentina.* Economic Geology, 98: 1535-1574.

Qiu, N.S., Zhang, S.W. & Jin, Z.J. 2001. *Migration models of hydrocarbon fluids in the Dongying depression-evidences from boiling fluid inclusions.* Petroleum Geology and Experiment, 23(4): 403-407(in Chinese with English abstract).

Roedder, E. & Bodnar, R.J. 1980. *Geologic pressure determinations from fluid inclusion studies*. Ann Rev Earth Plannet Sci, 8: 263-301.

Roedder, E. 1984. *Fluid inclusions*. Reviews in mineralogy. Mineral Soc. Amer., 12: 1-644.

Rui, Z.Y., Li, Y.Q. & Wang. L.S. 2003.*Approach to ore-forming conditions in light of ore fluid inclusions.* Mineral Deposits, 22(1): 13-23 (in Chinese with English abstract).

Shepherd, T.J., Rankin, A.H. & Alderton, D.H.M. 1985. *A Practical Guide to Fluid Inclusion Studies.* Blackie: Chapman and Hall. 1-239.

Wang, X.C., Wang, X.L., Wang, L., Liu, J.Y., Xia, B., Deng, J. & Xu, X.M. 2007. *Metallogeny and reformation of the Duobaoshan superlarge porphyry copper deposit in Heilongjiang.* Chinese Journal of Geology, 42(1): 124-133 (in Chinese with English abstract)

Wu, G., Liu, J., Zhong, W., Zhu, M.T., Mi, M. & Wan, Q. 2009. *Fluid inclusion study of the Tongshan porphyry copper deposit, Heilongjiang province, China.* Acta Petrologica Sinica, 25(11): 2995-3006 (in Chinese with English abstract).

Zhang, L.Y. 1989. *Theory and prospecting for diagenesis and ore-forming*. BeiJing: industry university of BeiJing, 189-190

Zhang, Y.G. & Frantz, J.D. 1987. *Determination of the homogenization temperatures and densities of supercritical fluids in the system $NaCl$-KCl-$CaCl_2$-H_2O using synthetic fluid inclusions.* Chem Geol, 64: 335-351.

Zhao, Y.M., Bi, C.S., Zou, X.Q., Sun, Y.L., Du, A.D. & Zhao, Y.M. 1997 *The Re-Os Isotopic Age of Molybdenite from Duobaoshan and Tongshan Porphyry Copper (Molybdenum) Deposits.* Acta Geoscientia Sinica, 18(1): 61-67 (in Chinese with English abstract).

Zhao, Y.M. & Zhang, D.Q. 1997. *Law and prospective evaluation of copper polymetallic deposit mineralization in Daxing'anling and its adjacent areas.* Beijing: Geology Publishing House, 40-80 (in Chinese).

Zhao, Y.Y., Ma, Z.H. & Zhong, C.X. 1997. *A study on ore-forming geochemistry of Duobaoshan copper deposit, Heilongjiang province.* Journal of Xi'an College of Geology, 19(1): 28-35 (in Chinese with English abstract).

Received at: 07. 11. 2013
Revised at: 08.07. 2014
Accepted for publication at: 01. 08. 2014
Published online at: 09. 08. 2014